

Effects of a Thermal Accelerant Gel on Microwave Ablation Zone Volumes in Lung: A Porcine Study


Aaron W. P. Maxwell, MD • William K. C. Park, PhD • Grayson L. Baird, PhD • Douglas W. Martin, MD • Kara A. Lombardo, BS • Damian E. Dupuy, MD

From the Department of Diagnostic Imaging, The Warren Alpert Medical School of Brown University, 593 Eddy St, Providence, RI 02903. Received July 13, 2018; revision requested August 23; revision received November 28; accepted December 21. Address correspondence to A.W.P.M. (e-mail: Aaron_Maxwell@brown.edu).

Study supported by Radiological Society of North America (grant number RR1702).

Conflicts of interest are listed at the end of this article.

See also the editorial by Goldberg in this issue.

Radiology 2019; 00:1–7 • <https://doi.org/10.1148/radiol.2019181652> • Content code: 

Background: Thermal ablation of cancers may be associated with high rates of local tumor progression. A thermal accelerant gel has been developed to improve the transmission of microwave energy in biologic tissues with the aim of enlarging the thermal ablation zone.

Purpose: To determine the effects of a thermal accelerant gel on microwave ablation zone volumes in porcine lung and to compare percutaneous and endobronchial delivery methods.

Materials and Methods: Thirty-two consecutive microwave lung ablations were performed in nine 12-week-old domestic male swine under general anesthesia by using fluoroscopic guidance between September 2017 and April 2018. Experimental ablations were performed following percutaneous injection of thermal accelerant into the lung ($n = 16$) or after endobronchial injection by using a flexible bronchoscope ($n = 8$). Control ablations were performed without accelerant gel ($n = 8$). Lung tissue was explanted after the animals were killed, and ablation zone volumes were calculated as the primary outcome measure by using triphenyltetrazolium chloride vital staining. Differences in treatment volumes were analyzed by generalized mixed modeling.

Results: Thermal accelerant ablation zone volumes were larger than control ablations (accelerant vs control ablation, 4.3 cm^3 [95% confidence interval: 3.4, 5.5] vs 2.1 cm^3 [95% confidence interval: 1.4, 2.9], respectively; $P < .001$). Among ablations with the thermal accelerant, those performed following percutaneous injection had a larger average ablation zone volume than those performed following endobronchial injection (percutaneous vs endobronchial, 4.8 cm^3 [95% confidence interval: 3.6, 6.4] vs 3.3 cm^3 [95% confidence interval: 2.9, 3.8], respectively; $P = .03$). Ablation zones created after endobronchial gel injection were more uniform in size distribution (standard error, percutaneous vs endobronchial: 0.13 vs 0.07, respectively; $P = .03$).

Conclusion: Use of thermal accelerant results in larger microwave ablation zone volumes in normal porcine lung tissue. Percutaneous thermal accelerant injection leads to a larger ablation zone volume compared with endobronchial injection, whereas a more homogeneous and precise ablation zone size is observed by using the endobronchial approach.

© RSNA, 2019

Image-guided thermal ablation achieves therapeutic oncology through the local application of extreme temperature, generating irreversible cell injury via the induction of coagulative necrosis and apoptosis (1). Early image-guided thermal ablation research focused on the use of radiofrequency energy for this purpose, whereas more recently interest in microwave energy has grown because of its association with larger ablation zones, faster tissue heating, and reduced susceptibility to heat-sink effects (2). Multiple large case series and systematic reviews and meta-analyses demonstrated compelling treatment results following ablation in solid organs such as the kidneys and liver, with patient outcomes often rivaling those achieved with surgical intervention (3–9).

Despite these successes, however, ablation remains a second-line therapy for most cancer types because of published high rates of local tumor progression. In lung, for example, 3-year local tumor progression rates after microwave ablation were recently reported (10) as high as 44% with an associated 11-fold decrease in the odds of primary technique efficacy for tumors larger than 3 cm. Similar

results were also previously published (11,12). These data emphasize the need for the development and optimization of alternative approaches to the nonoperative treatment of lung cancer, which remains the most common cause of cancer-related death among both men and women in the United States with a rising incidence (13,14).

To address these challenges, our laboratory has developed a thermal accelerant gel formulated to improve the transmission of microwave energy in biologic tissues. Preliminary in vivo trials have found a significant effect of thermal accelerant use in porcine muscle and liver, with observed ablation zone volume enlargement of 69.7% and 57.2%, respectively (15,16). To our knowledge, the thermal accelerant has not been previously evaluated in the lung, however, and its effects therein remain unknown.

On the basis of previous investigations, we hypothesize that the use of thermal accelerant will increase microwave ablation zone volumes in lung when compared with control ablations. We further hypothesize that the route of accelerant gel administration will influence treatment

Summary

In healthy porcine lung, the administration of a thermal accelerant gel before microwave ablation resulted in a larger ablation zone size compared with control ablations performed without thermal accelerant.

Key Points

- Use of thermal accelerant gel produced a greater than twofold increase in mean ablation zone volume versus no gel following microwave ablation in healthy lung tissue.
- Ablation zones created following endobronchial gel injection were more uniform in size distribution than those without endobronchial gel.
- Endobronchial administration of thermal accelerant gel improved ablation precision relative to percutaneous injection and may be a useful adjunct to endobronchial thermal ablation.

outcomes, with endobronchial delivery via bronchoscopy predicted to improve ablation zone precision compared with conventional percutaneous injection because of greater uniformity of gel deposition. Accordingly, the purpose of our investigation was to evaluate the effects of thermal accelerant gel use in the lung following microwave ablation and to assess potential differential effects of percutaneous and endobronchial administration methods by using a large animal model.

Materials and Methods

Thermal Accelerant

The thermal accelerant (Heatsync; Theromics, West Bridgewater, Mass) is a proprietary protein-based formulation that functions through the augmentation of microwave energy transmission in the region of the ablation antenna, leading to faster tissue heating, higher ablation zone temperature, and enhanced thermal cytotoxicity (15,16). The thermal accelerant exists as a translucent gel at both room and body temperature with a measured viscosity of $3.48 \text{ kg/m}^2/\text{sec} \pm 0.08$. To achieve sufficient radiodensity for targeting the thermal accelerant aliquot by using fluoroscopic guidance in the our investigation, the injection catheter was primed with 1 mL low-osmolar iodinated contrast material (Omnipaque 350; GE Healthcare, Chicago, Ill) before each administration of accelerant gel.

This study was performed between September 2017 and April 2018 after approval by institutional animal use and care committee. The thermal accelerant gel used in this study was supplied by Theromics. Authors not employed by or consultants for Theromics (A.W.P.M., G.L.B., D.W.M., and K.A.L.) had complete control over the inclusion of any data and information that might present a conflict of interest for those authors who are employees of or consultants for Theromics. These authors (A.W.P.M., G.L.B., D.W.M., and K.A.L.) also had full control of all data analysis and interpretation. W.K.C.P. is a paid employee of Theromics, and D.E.D. is an unpaid consultant.

In Vivo Microwave Ablation Experiments

Nine healthy 12-week-old castrated male domestic swine (45–50 kg) were used as model organisms because of their large

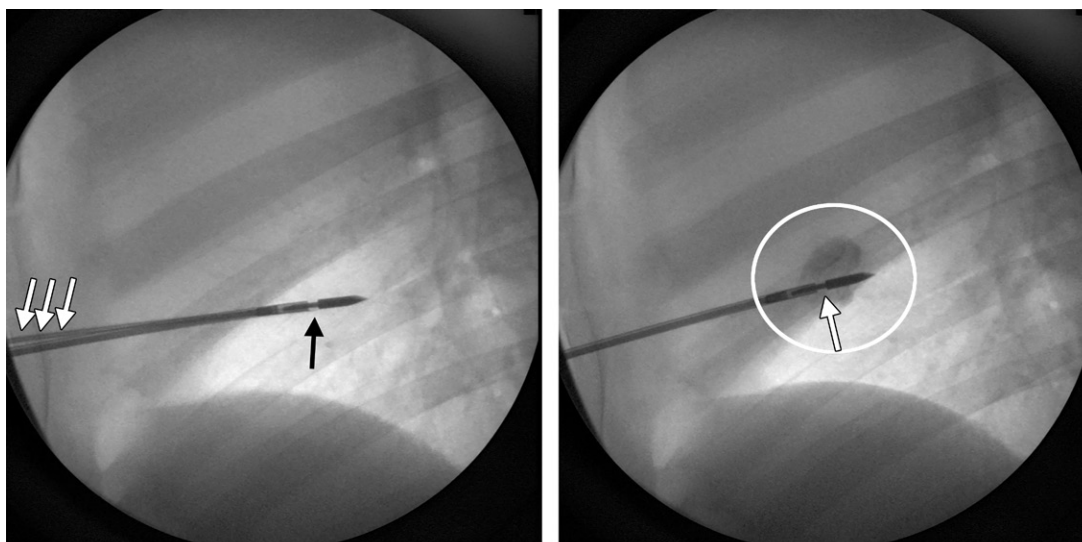
size and similar cardiopulmonary system to humans. All swine were housed in pairs within a dedicated animal research facility throughout a 48-hour acclimation period before ablation. Food and water were provided ad libitum until the midnight preceding the procedures, when animals were to take nothing by mouth. Ablations were performed in a dedicated large animal procedure suite.

For each procedure, general endotracheal anesthesia was administered under the guidance of a board-certified laboratory animal veterinarian with 15 years of experience by using 1%–4% inhaled isoflurane gas. Following induction, animals were placed in the supine position on the operating table and safely anchored with padded limb straps. Continuous cardiopulmonary monitoring including heart rate and rhythm, blood pressure, pulse oximetry, and end-tidal capnography was used for evaluation of animal hemodynamics and to facilitate real-time assessment of potential intra-procedural complications such as pneumothorax or hemorrhage.

Microwave ablations were performed by using the MicrothermX system (Perseon Medical, Salt Lake City, Utah) by one of two authors (A.W.P.M. and D.E.D., with 3 and 25 years of experience in image-guided tumor ablation, respectively). A single 10-cm short-tip antenna was used for each treatment at a power of 60 W and a frequency of 950 MHz for a duration of 10 minutes, parameters that were previously demonstrated to yield optimal augmentation of microwave energy conduction during *in vitro* thermal accelerant trials (16). Microwave antennae were percutaneously placed into healthy porcine lung tissue under fluoroscopic guidance that targeted areas remote from central bronchovascular structures and visceral pleural margins. For the purposes of this study, the lungs were grossly divided into quadrants without respect to lobar anatomy (ie, right and left, upper and lower) and a maximum of one ablation per quadrant was attempted in each animal. An injected gel volume of 2 mL was used for each thermal accelerant ablation, twice the volume used in previous *in vivo* trials in the liver (15) because of the expected dispersion of gel within the air-filled spaces of the lung.

Control ablations were performed without thermal accelerant according to our parameters, whereas experimental ablations were performed after percutaneous or endobronchial thermal accelerant delivery. For percutaneous ablations, a 10-cm 5-F catheter (Yueh; Cook Medical, Bloomington, Ind) was advanced over a needle into the lung and 2 mL of thermal accelerant were slowly injected under fluoroscopy. The microwave antenna was then percutaneously placed under fluoroscopy with the antenna feed point (1 cm proximal to tip) centrally positioned within the thermal accelerant deposit (Fig 1) by using orthogonal and oblique projections.

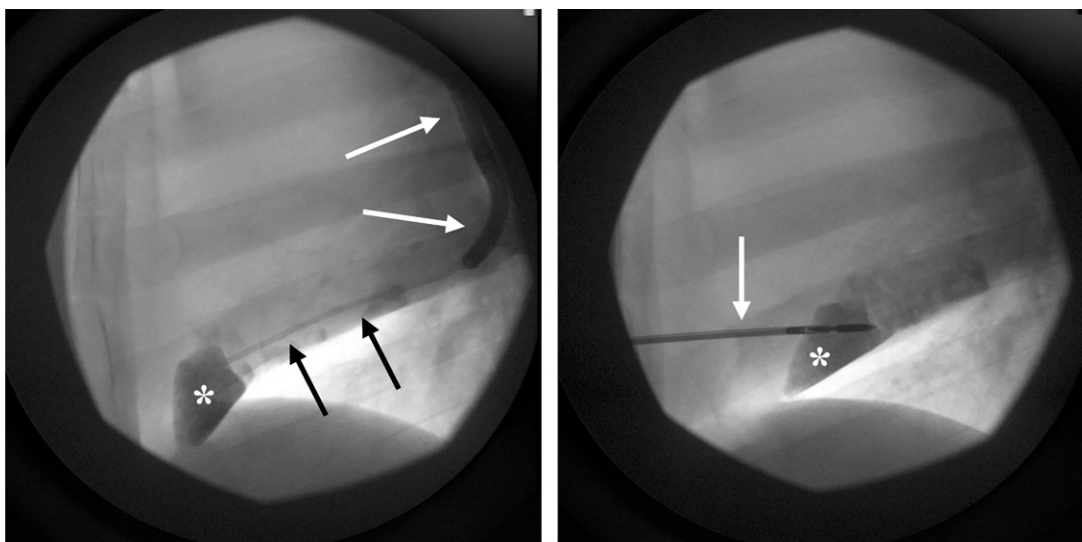
For endobronchial ablations, a flexible bronchoscope was placed into the tracheobronchial tree by a fellowship-trained pulmonologist (D.W.M., with 8 years of experience in endobronchial intervention). After the bronchoscope was navigated to the desired treatment location, a 60-cm 5-F endovascular catheter was introduced through a side port in the bronchoscope and advanced into the lung (Fig 2). As in the percutaneous delivery condition, 2 mL of thermal accelerant were slowly injected into the lung under fluoroscopy, after which



a.

b.

Figure 1: Spot fluoroscopic images obtained during percutaneous thermal accelerant administration and ablation. **(a)** A microwave antenna (black arrow) and 5-F catheter (white arrows) were inserted in tandem into the lung through the chest wall by using fluoroscopic guidance. **(b)** Thermal accelerant (circle) was then injected near the antenna feed point (arrow) and the catheter was removed before treatment.



a.

b.

Figure 2: Spot fluoroscopic images obtained during endobronchial thermal accelerant (*) administration and ablation. **(a)** A flexible bronchoscope (white arrows) was advanced into a lobar bronchus and a 5-F catheter (black arrows) was placed distally into the lung parenchyma. **(b)** The thermal accelerant was then slowly injected, and the bronchoscope and catheter were withdrawn and an ablation antenna (arrow) was advanced through the chest wall into the thermal accelerant aliquot.

the catheter and bronchoscope were completely removed from the animal's body. The microwave antenna was then percutaneously placed and ablation performed.

Ablation Zone Quantification

After completion of the ablation procedures, animals were humanely killed while undergoing general anesthesia by using an intravenous sodium pentobarbital solution (Fatal Plus; Vortech Pharmaceutical, Dearborn, Mich) administered by a veterinary

staff member. A sternotomy was then performed and the lungs resected en bloc for pathologic evaluation. Before disposal, the chest cavity was thoroughly inspected for evidence of hemorrhage (eg, hemothorax) or thermal injury to mediastinal structures such as the heart, great vessels, and central tracheobronchial tree. All explanted lung specimens were similarly assessed for nontarget ablation or other injuries before processing.

Ablation sites were externally identified postmortem by gross palpation and visual inspection, then manually sectioned

Microwave Ablation Zone Volumes and Lengths with and without Thermal Accelerant

Parameter	Control Ablation	Thermal Accelerant	<i>P</i> Value, Control versus Thermal Accelerant	<i>P</i> Value, Percutaneous versus Endobronchial
Volume (cm ³)	2.1 (1.4, 2.9)			.03*
Overall		4.3 (3.4, 5.5)	<.001	
Percutaneous		4.8 (3.7, 6.3)	<.001	
Endobronchial		3.3 (2.9, 3.8)	.01	
Long axis (mm)	1.7 (1.3, 2.3)			.17
Overall		2.2 (2.0, 2.4)	.04	
Percutaneous		2.2 (2.0, 2.5)	.04	
Endobronchial		2.0 (1.8, 2.3)	.19	
Short axis (mm)				.25
Overall	1.1 (0.8, 1.4)	1.5 (1.3, 1.8)	.02	
Percutaneous		1.6 (1.4, 1.9)	.15	
Endobronchial		1.5 (1.4, 1.6)	.14	

Note.—Data in parentheses are 95% confidence interval. *P* values less than .05 indicate statistical significance.

to an approximate thickness of 4 mm, with sections oriented along a plane perpendicular to the long axis of the microwave antenna tract by a certified technologist (K.A.L., with 5 years of experience). Each tissue sample was washed in a phosphate-buffered saline solution and immersed at 37°C in a light-blocked water bath containing 1% triphenyltetrazolium chloride vital staining solution (Sigma-Aldrich, St Louis, Mo) for 20 minutes, then fixed in formalin.

High-spatial-resolution digital imaging performed at a dedicated workstation with a measurement grid was used to determine ablation zone volume on a per-ablation basis, with nonviable lung tissue defined according to visual assessment of triphenyltetrazolium chloride stain positivity. Measurements were made by using commercially available digital image analysis software (Image Pro Premier v9.1; Media Cybernetics, Rockville, Md), and total ablation zone volume was calculated as the product of triphenyltetrazolium chloride staining area and section thickness, summed over the number of ablation zone sections. Long- and short-axis measurements were also made for each ablation. The long-axis measurement was defined according to the single greatest measurable dimension along a single section within the axial plane, and the short-axis was defined as the smallest measurable distance along a single section in a plane orthogonal to the long-axis dimension.

Statistical Analysis

A within-subjects experimental design was used to examine the effects of thermal accelerant administration and delivery method on ablation zone volume. Animals served as their own control subject, with both experimental (percutaneous and endobronchial) and control ablations performed in each animal. A partial Latin square design was used to control for potentially confounding effects related to physiologic differences in ventilation and perfusion between the upper and lower lung zones and differences between the right and left lungs based on the relative proximity of the microwave antenna to the cardiac blood pool and central vessels. Matched-pairs power analyses

were calculated for the difference between percutaneous and control ablations and between percutaneous and endobronchial ablations. Large effect sizes of 1.5 and 1.0 standard deviations for 90% and 80% power, respectively, were assumed, yielding a needed overall sample size of eight matches per analysis (32 total observations).

Generalized mixed modeling with sandwich estimation was used to evaluate the effect of treatment condition (thermal accelerant and no thermal accelerant) on the primary outcome measure of ablation zone volume.

Short- and long-axis ablation zone measurements were also assessed as a secondary outcome measure. Observations were nested within each animal assuming a lognormal distribution transformation. All statistical analyses were performed by using statistical software (SAS 9.4; SAS, Cary, NC) with PROC GLIMMIX. Significance was indicated at *P* value of .05, and all interval estimates were calculated for 95% confidence. Volume data are provided as natural log back-transformed estimates. The Dunnett-Hsu correction was used for multiple comparisons of the primary outcome measure, when appropriate, whereas long- and short-axis measurement comparisons were examined by using Tukey corrections.

Results

A total of 36 consecutive microwave ablation attempts were made in nine animals. Four technical failures occurred secondary to antenna malfunction ($n = 1$) or suboptimal opacification of the thermal accelerant ($n = 3$), yielding a final sample of 32 completed ablations (16 ablations percutaneous with accelerant, eight ablations endobronchial with accelerant, and eight control ablations without accelerant). Observations were evenly balanced between the right ($n = 16$) and left ($n = 16$) lungs and between the upper ($n = 16$) and lower ($n = 16$) lung zones. Data are summarized in the Table.

Compared with control ablations, the use of thermal accelerant (percutaneous or endobronchial) was associated with a larger average ablation zone volume (thermal accelerant, 4.3 cm³ [95% confidence interval: 3.4, 5.5]; control ablation, 2.1 cm³ [95% confidence interval: 1.4, 2.9]; $P < .001$) (Fig 3). This larger treatment volume relative to control ablations persisted when separately comparing percutaneous (4.8 cm³; 95% confidence interval: 3.7, 6.3) and endobronchial (3.3 cm³; 95% confidence interval: 2.9, 3.8) delivery methods with those ablations performed without thermal accelerant ($P < .001$ and $P = .02$, respectively).

Among ablations with thermal accelerant, the percutaneous administration of thermal accelerant resulted in larger ablation zones than in ablations performed after endobronchial delivery

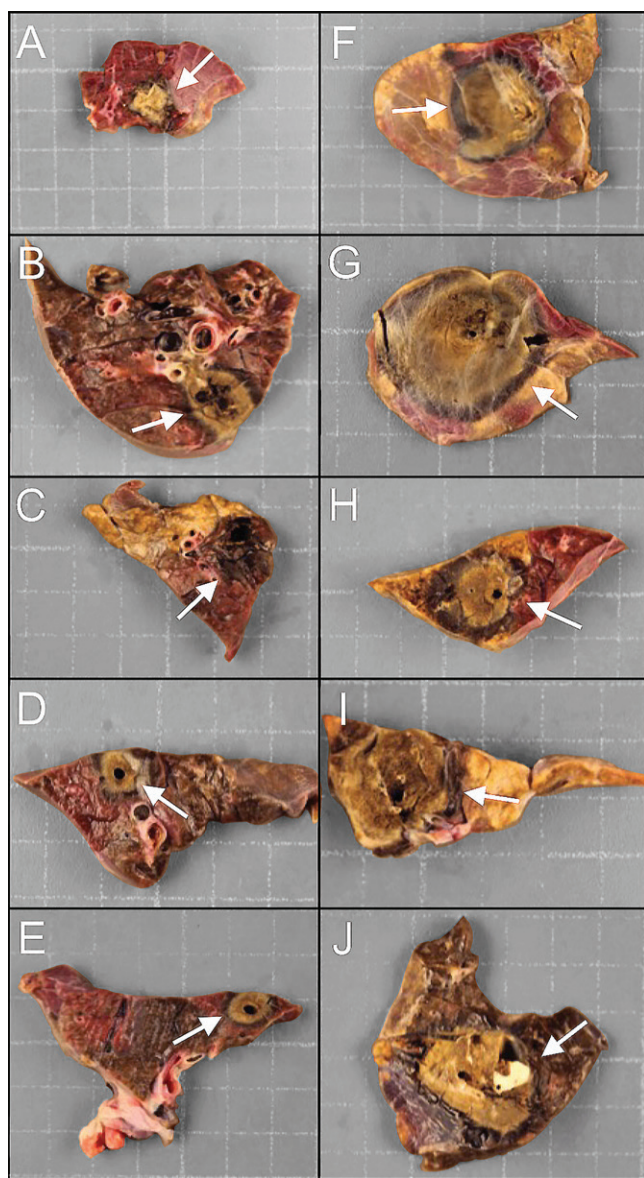


Figure 3: Gross porcine lung ablation specimens following triphenyltetrazolium chloride vital staining. When compared with, A–E, control ablations, the use of, F–J, thermal accelerant was greater in larger volumes of tissue necrosis (arrow).

(percutaneous administration, 4.8 cm^3 [95% confidence interval: 3.6, 6.4]; endobronchial administration, 3.3 cm^3 [95% confidence interval: 2.9, 3.8]; $P = .03$). However, endobronchial ablations showed greater precision than ablations performed following percutaneous administration of thermal accelerant, as evidenced by a lower standard error (endobronchial administration vs percutaneous administration standard error, 0.07 vs 0.13, respectively; $P = .03$), even as fewer observations were made in the endobronchial condition (eight vs 16 observations).

Differences in long- and short-axis ablation zone measurements were also evaluated. As detailed in the Table, the use of thermal accelerant gel resulted in greater enlargement of both axial measurement parameters compared with control ablations performed without the accelerant (long axis, $P = .04$; short axis, $P = .02$). No significant differences were observed regarding

long- and short-axis measurements when the percutaneous and endobronchial thermal accelerant injection groups were compared.

We did not observe adverse effects during any of the control or experimental microwave ablation treatments. Specifically, no pneumothoraces were identified, all nine animals remained hemodynamically stable, and none of the animals required premature euthanasia. No hemorrhage was identified at postmortem assessment, and there was no evidence of airway or cardiomedastinal injury in any animal.

Discussion

In our investigation, the effects of a thermal accelerant gel on microwave ablation zone volume were evaluated in nontumor-bearing porcine lung. Our results demonstrate that thermal accelerant use, on average, approximately doubles microwave ablation zone volumes (mean volume, 4.3 cm^3) in healthy lung tissue when compared with control ablations (mean volume, 2.1 cm^3). Because treatment failures after thermal ablation are known to primarily occur along the tumor periphery at sites of sublethal hyperthermia (17), the observed radial expansion of cytotoxic heating caused by administration of the accelerant gel suggests that its use in lung may be sufficient to reduce the rate of local tumor progression for lung tumors treated with image-guided thermal ablation.

We also investigated the effect of thermal accelerant delivery method on treatment outcomes. As we hypothesized, the percutaneous injection of thermal accelerant resulted in larger ablation zone volumes (mean volume, 4.8 cm^3) relative to control ablations. Ablations in the percutaneous accelerant group were also larger than those performed after endobronchial thermal accelerant injection (mean volume, 3.3 cm^3). Compared with the endobronchial approach (standard error, 0.07), however, percutaneous injection was associated with diminished treatment precision and a more inhomogeneous distribution of ablation zone volumes (standard error, 0.13).

This latter observation likely reflects the architectural complexity of lung tissue relative to solid organs, with both aerated and nonaerated spaces. Though percutaneous delivery of thermal accelerant can facilitate accurate and reproducible localization near the intended site of ablation, the deposited gel aliquot may demonstrate an unpredictable and irregular geometry because of atelectasis and local tissue trauma caused by needle placement (Fig 4). Conversely, endobronchial administration directly into the tracheobronchial tree can yield a more homogeneous and uniform distribution of gel deposition because of the atraumatic filling of alveoli and terminal bronchioles (Fig 5). This latter effect may improve reproducibility in ablation zone size and shape, and it may allow for more reliable postablation treatment margins, which are known to closely correlate with tumor recurrence risk and overall patient outcomes (18).

The observed success of endobronchial thermal accelerant injection may also prove relevant to the emerging trend of bronchoscopy-based thermal ablation techniques. As with other endobronchial interventions, a potential benefit of this approach is a lower rate of pulmonary hemorrhage and pneumothorax

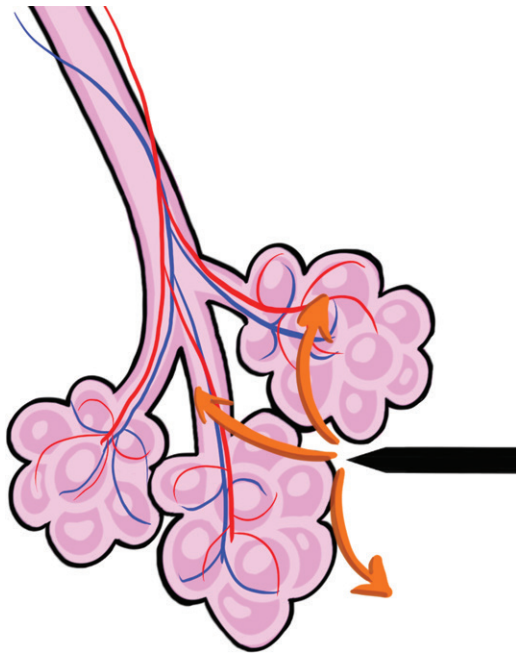


Figure 4: Schematic representation of percutaneous thermal accelerant gel administration. After advancing the needle into lung, thermal accelerant may disperse randomly within and around the intended site of deposition depending on the final location of the needle tip. The arrows represent the flow of thermal accelerant out of the injection catheter.

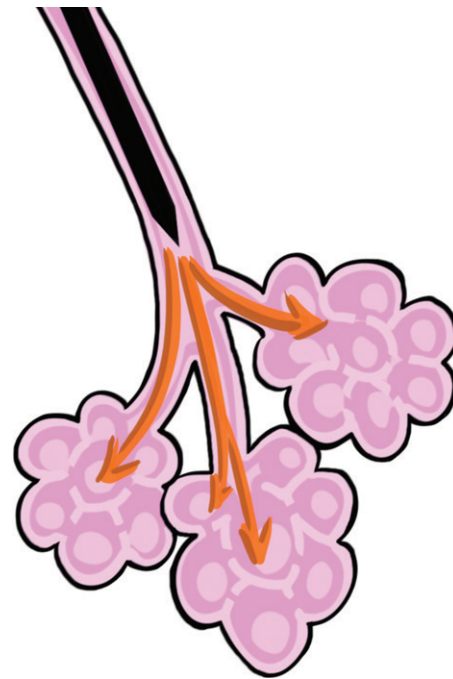


Figure 5: Schematic representation of endobronchial thermal accelerant gel administration. Bronchoscopic delivery would be expected to yield more uniform gel deposition within distal airways and alveolar sacs. The arrows represent the flow of thermal accelerant out of the injection catheter.

because of shorter intraparenchymal trajectory and lack of pleural puncture (19), and the potential for greater precision in lesion targeting by using electromagnetic navigation-based techniques (20). Several small case series that used endobronchial ablation have shown promising results, and one study (21) used radiofrequency energy and demonstrated a 35-month progression-free survival rate without any major adverse events, including pneumothorax, after treatment of 28 early stage non-small cell lung cancers. Endobronchial cryoablation has also been described for lung cancer treatment (22), and at least one endobronchial microwave ablation catheter is currently commercially available (23). Future studies evaluating the use of combined endobronchial ablation and thermal accelerant injection are planned by our own research group.

The lack of correlative data between temperature and ablation zone volume in this study deserves particular attention. The proposed mechanism of action for the thermal accelerant gel is improved microwave energy conduction and higher ablation zone temperature, and these produce a greater volume of coagulated tissue. Evidence in favor of this mechanism comes from prior *in vitro* work with the compound by using an agarose gel phantom model, wherein higher concentrations were associated with stepwise and reproducible temperature elevations beyond that achieved with a single microwave antenna (16). Nevertheless, the possibility of direct cytotoxic effects or other mechanisms such as immune stimulation (24) must be entertained, though this latter explanation is unlikely given the timing of animal sacrifice immediately following the ablation procedures.

There were several limitations to our study. Because normal healthy lung tissue was used, the observed ablation zone volume enlargement with thermal accelerant use may not have accurately reflected changes expected to occur in the presence of tumor cells. Specifically, because of the desmoplastic reaction incited by many primary lung cancers, there is likely to be altered microwave energy transmission within and surrounding the ablation zone, which may affect treatment outcomes. Because of sample size constraints, the identified effect sizes may not have accurately reflected the expected magnitude of change that would be observed on a population level. The lack of correlative CT data precluded detailed imaging assessment of the ablation zones. Finally, though no immediate complications were evident, conclusions regarding the presence or absence of potential long-term adverse effects of thermal accelerant use could not be rendered.

In summary, the *in vivo* administration of thermal accelerant into healthy swine lung compared with control ablations resulted in larger microwave ablation zone volumes. These effects were most pronounced when the thermal accelerant was percutaneously administered, whereas the direct administration of thermal accelerant into distal airways and alveolar spaces by using an endobronchial approach was associated with more uniform gel deposition and greater ablation zone volume precision.

Author contributions: Guarantors of integrity of entire study, A.W.P.M., W.K.C.P., D.E.D.; study concepts/study design or data acquisition or data analysis/interpretation, all authors; manuscript drafting or manuscript revision for important intellectual content, all authors; approval of final version of submitted manuscript, all authors; agrees to ensure any questions related to the work are appropriately resolved,

all authors; literature research, A.W.P.M., W.K.C.P., K.A.L., D.E.D.; clinical studies, D.E.D.; experimental studies, all authors; statistical analysis, A.W.P.M., G.L.B., K.A.L.; and manuscript editing, A.W.P.M., W.K.C.P., G.L.B., K.A.L., D.E.D.

Disclosures of Conflicts of Interest: **A.W.P.M.** Activities related to the present article: disclosed personal fees for employment from Theromics. Activities not related to the present article: disclosed patent pending for thermal accelerant compositions and methods of use by a license agreement with Theromics and Brown University. Other relationships: disclosed no relevant relationships. **W.K.C.P.** Activities related to the present article: disclosed that author is a paid employee of Theromics; disclosed money to author's institution for pending patents from Theromics and Lifespan for the thermal accelerant HeatSYNC used in this study. Activities not related to the present article: disclosed no relevant relationships. Other relationships: disclosed no relevant relationships. **G.L.B.** disclosed no relevant relationships. **D.W.M.** disclosed no relevant relationships. **K.A.L.** disclosed no relevant relationships. **D.E.D.** Activities related to the present article: disclosed money to author's institution for pending patents from Theromics and Lifespan for the thermal accelerant HeatSYNC used in this study. Activities not related to the present article: disclosed money paid to author from Perseon Medical for consultancy and payment for lectures including service on speakers bureaus; disclosed money to author's institution for patents from Lifespan Corporation for a thermal accelerant; disclosed royalties from Springer Verlag and Uptodate; disclosed payment for development of educational presentations from Lafrance for Society of Interventional Oncology. Other relationships: disclosed no relevant relationships.

References

1. Chu KF, Dupuy DE. Thermal ablation of tumours: biological mechanisms and advances in therapy. *Nat Rev Cancer* 2014;14(3):199–208.
2. Lubner MG, Brace CL, Hinshaw JL, Lee FT Jr. Microwave tumor ablation: mechanism of action, clinical results, and devices. *J Vasc Interv Radiol* 2010;21(8 Suppl):S192–S203.
3. Katsanos K, Mailli L, Krokidis M, McGrath A, Sabharwal T, Adam A. Systematic review and meta-analysis of thermal ablation versus surgical nephrectomy for small renal tumours. *Cardiovasc Intervent Radiol* 2014;37(2):427–437.
4. Xing M, Kokabi N, Zhang D, Ludwig JM, Kim HS. Comparative effectiveness of thermal ablation, surgical resection, and active surveillance for T1a renal cell carcinoma: a Surveillance, Epidemiology, and End Results (SEER)-Medicare-linked population study. *Radiology* 2018;288(1):81–90.
5. Rivero JR, De La Cerda J 3rd, Wang H, et al. Partial nephrectomy versus thermal ablation for clinical stage T1 Renal masses: systematic review and meta-analysis of more than 3,900 patients. *J Vasc Interv Radiol* 2018;29(1):18–29.
6. Yamashita YI, Imai K, Kaida T, et al. Multimodal radiofrequency ablation versus laparoscopic hepatic resection for the treatment of primary hepatocellular carcinoma within Milan criteria in severely cirrhotic patients: long-term favorable outcomes over 10 years. *Surg Endosc* 2018 Jun 5. [Epub ahead of print].
7. Mohkam K, Dumont PN, Manichon AF, et al. No-touch multipolar radiofrequency ablation vs. surgical resection for solitary hepatocellular carcinoma ranging from 2 to 5 cm. *J Hepatol* 2018;68(6):1172–1180.
8. Chong CCN, Lee KF, Chu CM, et al. Microwave ablation provides better survival than liver resection for hepatocellular carcinoma in patients with borderline liver function: application of ALBI score to patient selection. *HPB* 2018;20(6):546–554.
9. Chen MS, Li JQ, Zheng Y, et al. A prospective randomized trial comparing percutaneous local ablative therapy and partial hepatectomy for small hepatocellular carcinoma. *Ann Surg* 2006;243(3):321–328.
10. Healey TT, March BT, Baird G, Dupuy DE. Microwave ablation for lung neoplasms: a retrospective analysis of long-term results. *J Vasc Interv Radiol* 2017;28(2):206–211.
11. Belfiore G, Ronza F, Belfiore MP, et al. Patients' survival in lung malignancies treated by microwave ablation: our experience on 56 patients. *Eur J Radiol* 2013;82(1):177–181.
12. Vogl TJ, Worst TS, Naguib NN, Ackermann H, Gruber-Rouh T, Nour-Eldin NE. Factors influencing local tumor control in patients with neoplastic pulmonary nodules treated with microwave ablation: a risk-factor analysis. *AJR Am J Roentgenol* 2013;200(3):665–672.
13. Rahib L, Smith BD, Aizenberg R, Rosenzweig AB, Fleshman JM, Matrisian LM. Projecting cancer incidence and deaths to 2030: the unexpected burden of thyroid, liver, and pancreas cancers in the United States. *Cancer Res* 2014;74(11):2913–2921.
14. Siegel RL, Miller KD, Jemal A. Cancer statistics, 2018. *CA Cancer J Clin* 2018;68(1):7–30.
15. Park WK, Maxwell AW, Frank VE, et al. The in vivo performance of a novel thermal accelerant agent used for augmentation of microwave energy delivery within biologic tissues during image-guided thermal ablation: a porcine study. *Int J Hyperthermia* 2018;34(1):11–18.
16. Park WK, Maxwell AW, Frank VE, et al. Evaluation of a novel thermal accelerant for augmentation of microwave energy during image-guided tumor ablation. *Theranostics* 2017;7(4):1026–1035.
17. Brace CL. Radiofrequency and microwave ablation of the liver, lung, kidney, and bone: what are the differences? *Curr Probl Diagn Radiol* 2009;38(3):135–143.
18. Anderson EM, Lees WR, Gillams AR. Early indicators of treatment success after percutaneous radiofrequency of pulmonary tumors. *Cardiovasc Intervent Radiol* 2009;32(3):478–483.
19. Vieira T, Stern JB, Girard P, Caliendo R. Endobronchial treatment of peripheral tumors: ongoing development and perspectives. *J Thorac Dis* 2018;10(Suppl 10):S1163–S1167.
20. Xie F, Zheng X, Xiao B, Han B, Herth FJF, Sun J. Navigation bronchoscopy-guided radiofrequency ablation for nonsurgical peripheral pulmonary tumors. *Respiration* 2017;94(3):293–298.
21. Koizumi T, Tsushima K, Tanabe T, et al. Bronchoscopy-guided cooled radiofrequency ablation as a novel intervention therapy for peripheral lung cancer. *Respiration* 2015;90(1):47–55.
22. Schumann C, Hetzel M, Babiak AJ, et al. Endobronchial tumor debulking with a flexible cryoprobe for immediate treatment of malignant stenosis. *J Thorac Cardiovasc Surg* 2010;139(4):997–1000.
23. Medwaves, Inc Web site. <http://www.medwaves.com/>. Accessed November 23, 2018.
24. Waitz R, Solomon SB, Petre EN, et al. Potent induction of tumor immunity by combining tumor cryoablation with anti-CTLA-4 therapy. *Cancer Res* 2012;72(2):430–439.